01 Mar 2022

Investigation of Mechanical Properties of Parts Fabricated with Gas- and Water-Atomized 304L Stainless Steel Powder in the Laser Powder Bed Fusion Process

M. Hossein Sehhat

Austin T. Sutton

Chia Hung Hung

Joseph William Newkirk
Missouri University of Science and Technology, jnewkirk@mst.edu

et. al. For a complete list of authors, see https://scholarsmine.mst.edu/matsci_eng_facwork/2893

Recommended Citation

M. H. Sehhat et al., "Investigation of Mechanical Properties of Parts Fabricated with Gas- and Water-Atomized 304L Stainless Steel Powder in the Laser Powder Bed Fusion Process," *JOM*, vol. 74, no. 3, pp. 1088 - 1095, Springer; Minerals, Metals and Materials Society (TMS), Mar 2022.
The definitive version is available at https://doi.org/10.1007/s11837-021-05029-7

JOM, Vol. 74, No. 3, 2022
https://doi.org/10.1007/s11837-021-05029-7

Investigation of Mechanical Properties of Parts Fabricated with Gas- and Water-Atomized 304L Stainless Steel Powder in the Laser Powder Bed Fusion Process

M. HOSSEIN SEHHAT,[1,5] AUSTIN T. SUTTON,[2] CHIA-HUNG HUNG,[3] JOSEPH W. NEWKIRK,[4] and MING C. LEU[1]

1.—Department of Mechanical and Aerospace Engineering, Missouri University of Science and Technology, Rolla, MO 65409, USA. 2.—Los Alamos National Laboratory, Los Alamos, NM 87545, USA. 3.—Department of Mechanical Engineering, National Cheng Kung University, Tainan, Taiwan. 4.—Department of Materials Science and Engineering, Missouri University of Science and Technology, Rolla, MO 65409, USA. 5.—e-mail: hsehhat@mst.edu

The use of gas-atomized powder as the feedstock material for the laser powder bed fusion (LPBF) process is common in the additive manufacturing (AM) community. Although gas-atomization produces powder with high sphericity, its relatively expensive production cost is a downside for application in AM processes. Water atomization of powder may overcome this limitation due to its low cost relative to the gas-atomization process. In this work, gas- and water-atomized 304L stainless steel powders were morphologically characterized through scanning electron microscopy (SEM). The water-atomized powder had a wider particle size distribution and exhibited less sphericity. Measuring powder flowability using the Revolution Powder Analyzer (RPA) indicated that the water-atomized powder had less flowability than the gas-atomized powder. Through examining the mechanical properties of LPBF fabricated parts using tensile tests, the gas-atomized powder had significantly higher yield tensile strength and elongation than the water-atomized powder; however, their ultimate tensile strengths were not significantly different.

INTRODUCTION

Part fabrication using conventional manufacturing methods has several limitations. Parts with complex geometry have to be manufactured in several steps, including assembly and welding,[1] which require more material and labor cost. Also, to produce parts with free-form geometries, the material's formability is a limiting factor, during both design and production steps.[2] Although new techniques have been innovated to resolve such challenges, the appearance of defects in fabricated parts is still inevitable.[3,4] The development of additive manufacturing (AM) in the past decade has eliminated several of these challenges through part fabrication in a layer-by-layer manner. In nearly all AM processes, the characteristics of the feedstock material play a significant role in final part properties.[5,6,7] Powder material as the feedstock for several additive manufacturing processes is important from various viewpoints, such as powder flow properties, impact on the mechanical properties of fabricated parts, and economic consideration.[8,9] In the laser powder bed fusion (LPBF) process the feedstock material is in the form of powder with some specific characteristics such as particle size and size distribution, particle geometry, and powder flowability.[10] Also, recently, powder spreadability, which is a function of all the mentioned powder characteristics, has been found to play an important role in the LPBF process.[11] The characteristics of the feedstock powder significantly influences the fabricated parts' microstructure and mechanical properties.[12,13] Gas-atomized powder has been found to result in better mechanical properties

(Received September 15, 2021; accepted November 4, 2021; published online December 2, 2021)

when compared with the powders produced by other powder production methods including water atomization and mechanical crushing.[14] The particles in gas-atomized powder have spherical geometries without fine satellite particles, resulting in better flow properties due to lower inter-particle friction. Such merits that have made the gas-atomized powder commonly used in the AM field come with an expensive price due to the high cost of inert gas media used for gas-atomized powder production.[15] If a powder type capable of providing comparable mechanical properties at a cheaper price is implemented as the feedstock for the LPBF process, there would be a significant economic benefit.

Water-atomization is a process similar to gas-atomization, except that the powder is exposed to water instead of an inert gas.[16] As a potential substitution of feedstock material, water-atomized powder may be attractive because of its much cheaper price than gas-atomized powder. Utilization of water instead of an inert gas decreases the powder price by about one half for 304L SS powder. However, the properties of the generated powder particles are different.[17] It has been shown from powder morphology that water-atomized powder is not as desirable as gas-atomized powder.[18] However, more research is needed to compare the mechanical properties of AM parts corresponding to each type of powder.

In this work, the 304L SS powders produced by both gas-atomization and water-atomization processes were studied to correlate the powder characteristics to the mechanical properties of parts fabricated by the LPBF process. The particles' morphology was investigated using scanning electron microscopy (SEM), the powder flowability was assessed using a Revolution Powder Analyzer, and the fabricated parts' mechanical properties were measured using tensile tests. The rest of the paper is organized as follows. Section 2 describes the materials and methods used for powder characterization, part fabrication, and tensile testing. Section 3 discusses the results for the two different powder types in terms of morphology and flowability, and the mechanical properties of LPBF fabricated parts. Section 4 draws the conclusion of this study.

MATERIALS AND METHODS

Materials

The argon gas-atomized and water-atomized 304L stainless steel (SS) powders were provided by LPW Technology (Carpenter Technology Corp., USA). The initial particle size provided by the powder manufacturer was in the range of 15–45 μm for gas-atomized powder and 12–57 μm for water-atomized powder.

Measurement Equipment

The LPBF machine used in this study was a Renishaw AM250 (Renishaw plc., UK), which is capable of fabricating parts with complex geometries from a variety of metal powders. This machine is equipped with a high-precision (70-μm focal diameter) 200-W fiber laser and a build volume of $250 \times 250 \times 300$ mm^3. It has a powder recovery system (sieve, for particle size < 63 μm), which was used to eliminate the larger sized particles that had agglomerated during material handling. Tensile testing of the mechanical properties of the fabricated parts was performed using an Instron 5969 Dual Column Universal Testing System (Instron, USA) with 50-kN force capacity. The ASPEX Personal SEM (PSEM) (Aspex Corp., USA), which provides an automated feature analysis (AFA) option to reduce the time for analyzing the resulting micrographs, was utilized for powder characterization. The SEM device is capable of measuring the size, geometry, and chemical composition of thousands of particles in a short time (< 5 h). The powder flow properties were measured and analyzed using a Revolution Powder Analyzer (RPA) (Mercury Scientific Inc., USA). A wire electrical discharge machine (EDM) (Sodick Co., Japan) was used to cut the fabricated parts for preparing tensile specimens.

Powder Characterization

A main aspect of powder material is its morphology, which can be investigated in terms of particle shape, size, and size distribution.[19] Sieve analysis, microscopy, and laser diffraction are some of the existing methods for characterizing powder morphology.[20] The longer measurement times and unacceptable uncertainties of sieve analysis, and the measurement dependency on instrument design in laser diffraction make these two techniques ineffective, while SEM can be used to reliably analyze particle size and shape from a quantitative standpoint.[21] Thus, in this study, morphology analysis was performed by evaluation of SEM micrographs. To have the same basis of comparison between gas-atomized and water-atomized powders, both powders were sieved using a screen that passed particles with sizes smaller than 63 μm. In the evaluation, a thin layer of powder with roughly 20,000 particles was deposited on a carbon tape, attached to the top of a Bakelite mount, and grounded using a copper strip. The prepared samples were then evaluated with the ASPEX microscope, with several images at different locations of the captured powder. The images were analyzed using a MATLAB program to investigate the powder's particle size, size distribution, and aspect ratio.

The other powder characteristic studied was the powder's flowability. Powder flowability plays an important role in a powder's performance, especially where the particle size and shape vary depending on the material type.[22] Several powder flowability metrics, including Hall flowmeter measurements[23] and the angle of repose,[24] consider powder material in a static manner. However, powder in additive manufacturing processes behaves in a dynamic manner when the powder is being spread during the AM process. For this reason, a flowability metric that could represent powder's dynamic behavior would be a better representation of powder's flow properties for AM studies. The Revolution Powder Analyzer (RPA) is such an instrument. It is composed of a rotating drum with maximum volume capacity of 500 cm^3, and its measurement is done by a digital camera on the front side while the drum is illuminated from the back.[25] RPA software quantifies powder behavior from images taken by the digital camera. While this product can measure powder flowability using several metrics, the avalanche angle and break energy were used in this study. The same volume of each powder was fed into the instrument and the powder mass was used in the software for analysis.

Part Fabrication

To investigate the effect of material type on mechanical properties, 15 simple cubes with each edge of 10 mm were selectively laser melted for both gas-atomized and water-atomized powders using the Renishaw AM250 machine, using a laser power of 200 W and layer thickness of 50 μm. The layout of these cubes on the build plate is shown in Fig. 1. All values of the process parameters were kept the same for both powder types.

Figure 2a and b show the cubes fabricated from gas-atomized powder and water-atomized powder, respectively. The better properties of gas-atomized powder resulted in 15 fully spaced cubes, while the third row of cubes from water-atomized powder could not be fully fabricated. The 10 cubes obtained from water-atomized powder in the first and second rows were used for comparison with the cubes obtained from gas-atomized powder.

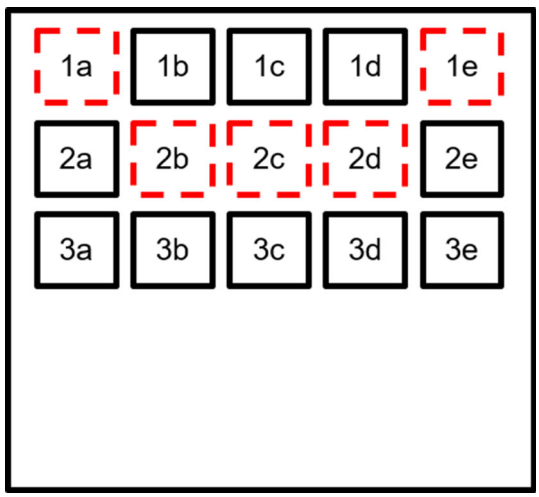

Fig. 1. Layout of parts on the build plate of Renishaw AM250 machine.

Tensile Tests

To prepare tensile specimens, the Sodick wire EDM machine was used to cut the cubes according to the standard tensile bar dimensions as shown in Fig. 3a. Six specimens were cut out of cubes shown in red in Fig. 1 to provide six replications for tensile testing. The specimens were cut out of the cubes in the first and second rows. The wire EDM process generated a heat affected zone (HAZ) on the specimen surface, which might affect the measured mechanical properties. Therefore, both sides of each tensile specimen were polished with a 600-grit sandpaper to remove the HAZ. Figure 3b shows the test specimens before and after polishing. The tensile tests were performed at room temperature with a crosshead speed of 0.015 mm/mm/min (strain rate per minute).[26]

RESULTS AND DISCUSSION

Powder Morphology

The SEM images in Fig. 4 show that the gas-atomized powder particles are much more spherical, while water-atomized powder particles have much more irregular shapes. Some of the particles in the gas-atomized powder Fig. 4a are the result of agglomeration, i.e., some particles combine to form larger particles. Also, some particles have cavities on the surface, probably due to collision between particles. The particles of water-atomized powder Fig. 4b have many different shapes, and their sizes vary massively from particle to particle.

Analyzing the SEM images provided data on the size, size distribution, and aspect ratio of powder particles. Figure 5 compares powder morphology between the water-atomized and gas-atomized powders in terms of particle size in 5(a) and aspect ratio in 5(b). Figure 5a shows the cumulative percentage of particle size, indicating that the water-atomized powder has more fine particles and wider size distribution. For example, the gas-atomized powder has D10 = 13.4 μm, i.e., 10% of the total number of particles are smaller than 13.4 μm; in comparison, D10 = 3.33 μm for the water-atomized powder. The size distributions of the two powders are also given in Table I with the values of D10, D50, and D90. The value of D50 for the water-atomized powder is 11.7 μm, which is smaller than that of the gas-atomized powder at 19.9 μm, which is due to the existence of considerably finer particles in the water-atomized powder.

Aspect ratio is one of the most commonly used particle shape representation factors. It is a

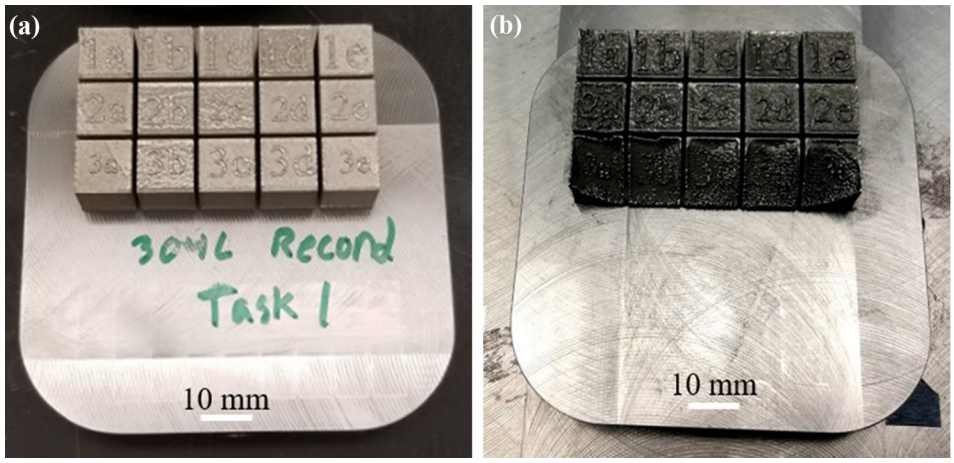

Fig. 2. Fabricated parts using (a) gas-atomized powder, and (b) water-atomized powder. The water-atomized powder did not result in fully fabricated cubes in the *third row*.

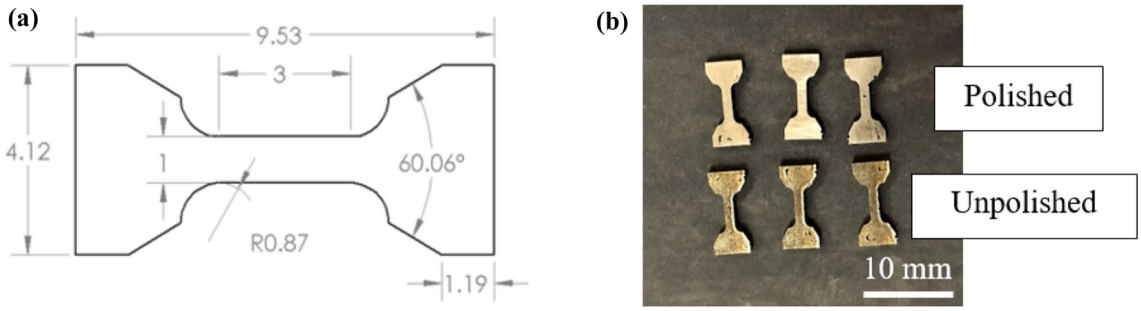

Fig. 3. Fabricated tensile test specimens (a) dimensions (unit: mm) of the test specimens,[27] (b) the test specimens before polishing (bottom row) and after polishing (top row).

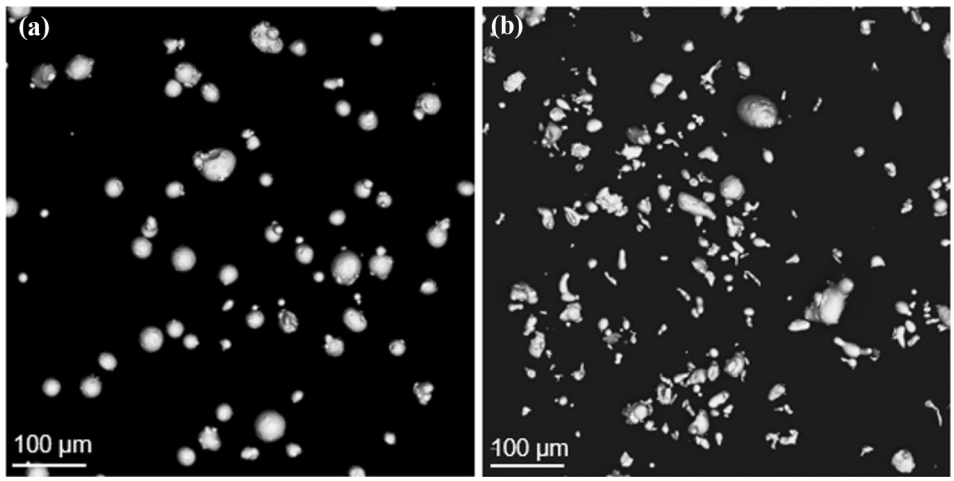

Fig. 4. Comparison between gas-atomized and water-atomized powder in terms of particle geometry: (a) gas-atomized powder, (b) water-atomized powder.

dimensionless factor defined as the ratio of the major axis to the minor axis of the bounding ellipse for a given particle.[28] Using this definition, the particle sphericity increases as the aspect ratio approaches unity. Figure 5b compares the cumulative number percentage vs aspect ratio for the gas-atomized and water-atomized powders. Approximately 65% of the gas-atomized powder particles have aspect ratios smaller than 1.2, while the corresponding value is 20% for the water-atomized powder particles. This considerable difference is indicative of the relative geometry irregularity in the water-atomized powder particles.

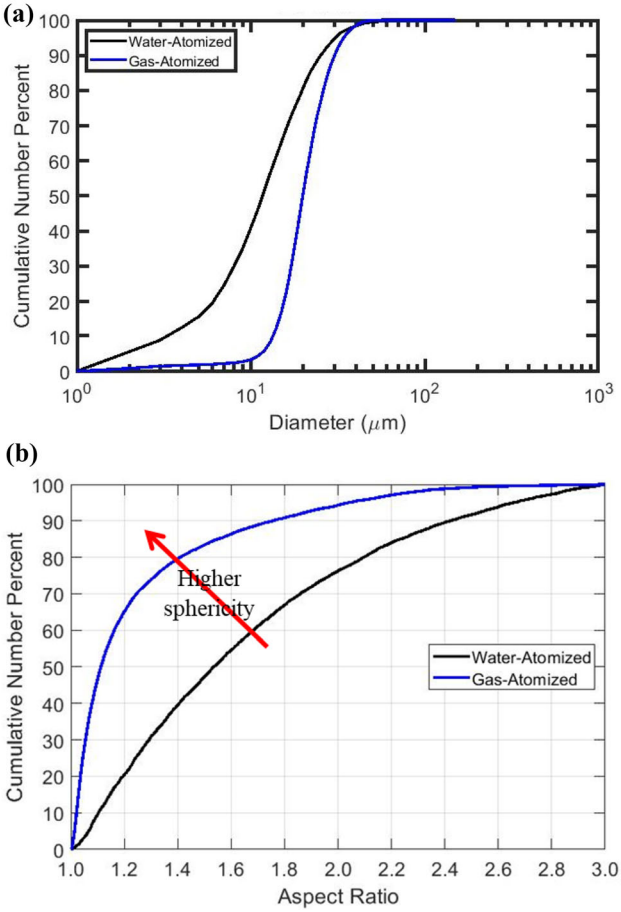

Fig. 5. Powder morphology comparison between the water-atomized and gas-atomized powders in terms of (a) particle size and (b) aspect ratio.

Table I. Size distributions of gas-atomized and water-atomized powders

Sample	D10	D50	D90
Gas-atomized powder	13.4	19.9	30.4
Water-atomized powder	3.33	11.7	25.3

Powder Density and Flowability

The metrics used for dynamic flow characteristics of a powder are avalanche angle and break energy, which can be measured using the Revolution Powder Analyzer (RPA). As the RPA's drum rotates, the inter-particle friction causes the powder to mimic a solid state initially. At a certain angle, the weight of powder overcomes its internal friction, causing the powder to slump, which is an avalanche. The maximum angle the powder pile makes before slumping is termed the avalanche angle. The break energy is a measure of the amount of energy needed to start an avalanche compared with the powder at a rest state. The rest energy is computed by measuring the potential energy of the powder before the drum is rotated. Then, the energy of the powder right before slumping is subtracted from the rest energy to obtain the break energy.

The results of flowability measurements for both powders are shown in Table II. Due to the larger avalanche angle and break energy, the water-atomized powder is clearly less flowable than the gas-atomized powder, due to the higher internal friction among the particles of water-atomized powder. The larger internal friction ultimately causes the water-atomized powder to pack less efficiently, resulting in a decrease in powder flowability. In general, as the particle size of a powder decreases, the flowability worsens from the increase in the adhesive force relative to the particle weight.[29] This is in good agreement with the result of our study. The smaller particle size and wider size distribution of water-atomized powder particles compared with those of gas-atomized powder resulted in a higher avalanche angle and a larger break energy, hence less flowability. The lower flowability of water-atomized powder was confirmed by the inability of the AM250 machine to fabricate complete cubes on the third row of the design layout see Fig. 2b. However, it is still unclear how the change in powder flowability will cause differences in the properties of fabricated parts. Therefore, the mechanical properties of parts fabricated by the LPBF process from the two types of powder will be compared and discussed in the next Section.

Mechanical Properties

The tensile test data we obtained to compare mechanical properties were yield strength (YS), ultimate tensile strength (UTS), and elongation. An ANOVA with significance level of $\alpha = 0.05$ was conducted on the data using Minitab software. A Tukey test was used for pairwise comparison between the mechanical properties of the gas-atomized (GA) powder and the water-atomized (WA) powder.

Before comparing the mechanical properties of the two types of powder, it should be noted that when comparing two properties, the difference is regarded as significant if the *P*-value of ANOVA is less than 0.05. For the Tukey comparison, it should be noted that two properties are significantly different if the 95% confidence interval of the two properties does not cross the zero line. Figure 6a shows the boxplots and Figure 6b depicts the Tukey comparison for the mean YS values of the two powders. The mean YS of the gas-atomized powder was 507 MPa, which was significantly larger than the mean YS of water-atomized powder at 470 MPa. The significance in the difference between these two values is confirmed by the *P*-value (< 0.5) of ANOVA and also by the Tukey comparison, which shows that the 95% confidence interval of the two mean YS values does not cross the zero line.

Table II. Dynamic flow properties of gas-atomized and water-atomized powders

Sample	Avalanche angle (°)	Break energy (mJ/kg)
Gas-atomized powder	34.8 ± 0.01	26.3 ± 0.74
Water-atomized powder	47 ± 0.03	48.7 ± 5.30

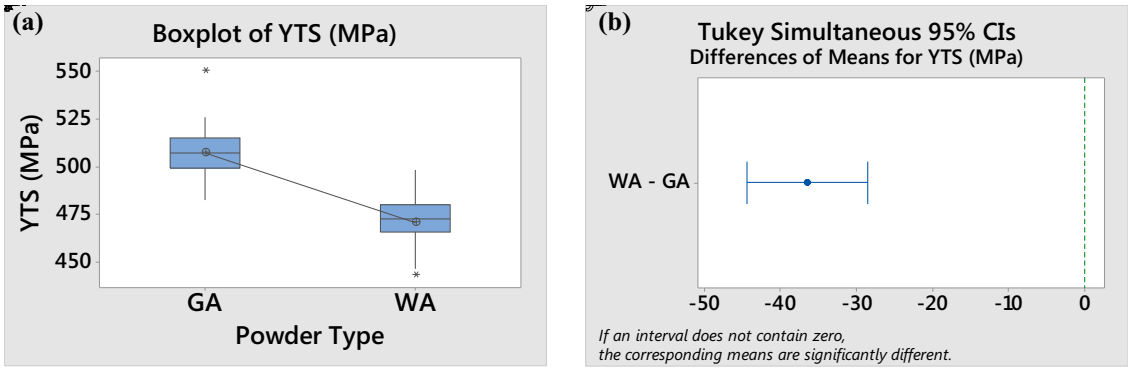

Fig. 6. Comparison between gas-atomized and water-atomized powder in terms of yield tensile strength: (a) mean boxplots, (b) Tukey comparison.

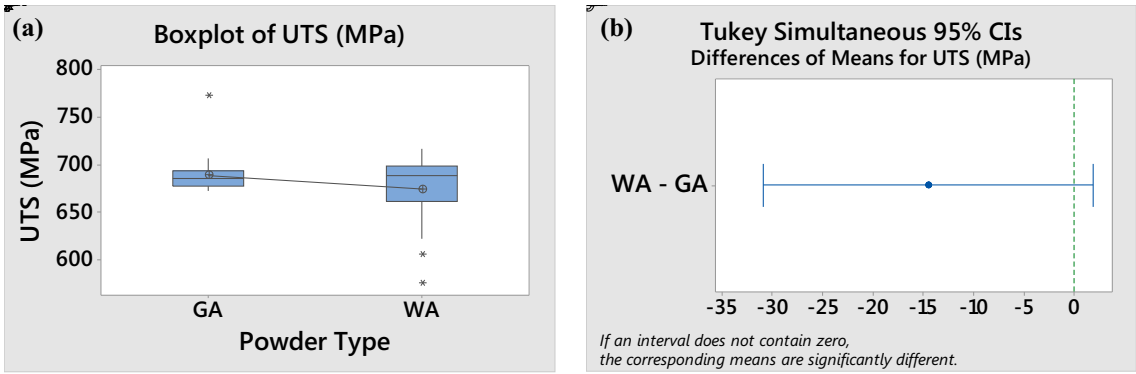

Fig. 7. Comparison between gas-atomized and water-atomized powder in terms of ultimate tensile strength: (a) mean boxplots, (b) Tukey comparison.

Interestingly, the null hypothesis of equal means for the UTS values of the two different powders could not be rejected, i.e., there is no significant difference in terms of the UTS values for the parts fabricated with the gas-atomized and water-atomized powders because the *P*-value = 0.08. The measured UTS values are shown in Fig. 7a for the boxplots and 7(b) for Tukey comparison. The UTS values for the gas-atomized and water-atomized powders were 688 MPa and 674 MPa, respectively, which are not significantly different given the confidence level of 95%. This can also be seen from the Tukey comparison, which shows that the 95% confidence interval of the two mean UTS values crosses the zero line.

The other mechanical property we compared was elongation, i.e., strain at break. The mean elongation value for gas-atomized powder was 0.69 while that of water-atomized powder was 0.29. The *P*-value of ANOVA on elongation was less than 0.05, indicating that the difference in elongation values among the samples fabricated from gas-atomized powder and water-atomized powder was statistically significant. The boxplots of elongation are shown in Fig. 8a and the Tukey comparison is shown in Fig. 8b. The interval of the mean elongation values at the 95% confidence level for the two powders does not cross the zero line, indicating that the two mean strains at break are significantly different.

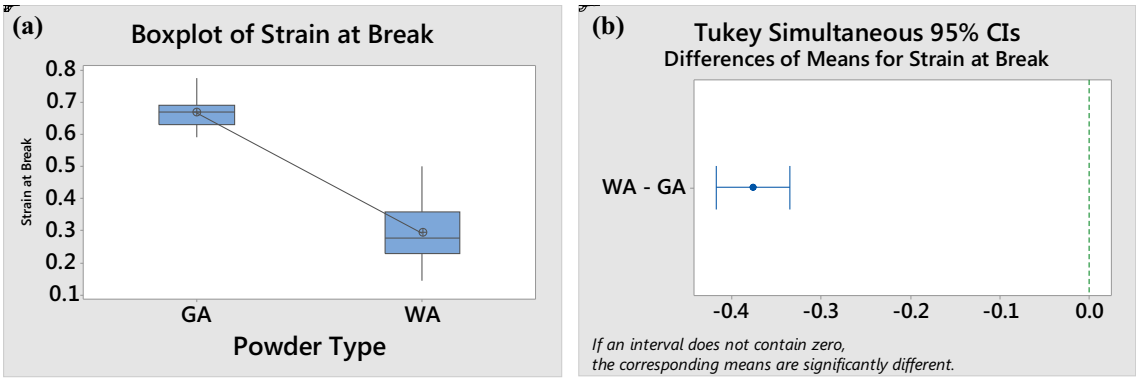

Fig. 8. Comparison between gas-atomized and water-atomized powder in terms of strain at break, (a) mean boxplots, (b) Tukey comparison.

CONCLUSION

In this study we compared gas-atomized and water-atomized SS 304L powders in terms of morphology, flowability, and mechanical properties of parts fabricated by the LPBF process with these two types of powder. It was found that water-atomized powder was much less spherical, and had a wider size distribution, with a larger number of fine particles than gas-atomized powder. The fine and irregularly shaped particles cause higher internal friction among powder particles, thus decreasing the powder flowability. The lower flowability was confirmed by the RPA measurement results, which showed that water-atomized powder had a higher avalanche angle and larger break energy compared with gas-atomized powder. Through standard tensile tests on fabricated specimens from both types of powder, it was observed that the powder type (gas-atomized vs water-atomized) had statistically significant effects on YS and elongation of the LPBF parts, i.e., gas-atomized powder results in significantly higher YS and elongation than water-atomized powder. However, the UTS difference between the parts fabricated from the two different types of powder is not statistically significant at the 95% confidence level.

ACKNOWLEDGEMENTS

This work was funded by Honeywell Federal Manufacturing & Technologies under Contract No. DE-NA0002839 with the U.S. Department of Energy. The United States Government retains, and the publisher, by accepting the article for publication, acknowledges that the United States Government retains a nonexclusive, paid up, irrevocable, worldwide license to publish or reproduce the published form of this manuscript, or allow others to do so, for United States Government purposes.

CONFLICT OF INTEREST

On behalf of all authors, the corresponding author states that there is no conflict of interest.

REFERENCES

1. A. Mahdianikhotbesara, M.H. Sehhat, and M. Hadad, *Metallogr. Microstruct. Anal.* 10, 1 (2021).
2. D. Rahmatabadi, M. Tayyebi, N. Najafizadeh, R. Hashemi, and M. Rajabi, *Mater. Sci. Technol.* 37, 1 (2021).
3. N. Najafizadeh, M. Rajabi, R. Hashemi, and S. Amini, *Proc. Inst. Mech. Eng. Part C J. Mech. Eng. Sci.* https://doi.org/10.1177/09544062211011509 (2021).
4. N. Najafizadeh, M. Rajabi, R. Hashemi, and S. Amini, *J. Theor. Appl. Vib. Acoust.* 5(1), 1 (2019).
5. C.H. Hung, W.T. Chen, M.H. Sehhat, and M.C. Leu, *Int. J. Adv. Manuf. Technol.* 112, 1 (2020).
6. B. Behdani, M. Senter, L. Mason, M. Leu, and J. Park, *J. Manuf. Mater. Process.* 4(2), 46 (2020).
7. M. H. Sehhat, B. Behdani, C.-H. Hung, and A. Mahdianikhotbesara, *Metallogr. Microstruct. Anal.* https://doi.org/10.1007/s13632-021-00795-x (2021).
8. P.D. Nezhadfar, S. Thompson, A. Saharan, N. Phan, and N. Shamsaei, *Miner Metals Mater Ser* 6, 212 (2021).
9. A.P. Jirandehi, M. Mehdizadeh, and M.M. Khonsari, *Int. J. Mech. Sci.* 176, 105525 (2020).
10. M. Moghadasi, W. Du, M. Li, Z. Pei, and C. Ma, *Ceram Int.* 46(10), 16966 (2020).
11. M.H. Sehhat, and A. Mahdianikhotbesara, *Granul. Matter.* 23, 1 (2021).
12. A.P. Jirandehi, and M.M. Khonsari, *Fatigue Fract. Eng. Mater. Struct.* 13515 (2021).
13. J.C. Simmons, X. Chen, A. Azizi, M.A. Daeumer, P.Y. Zavalij, G. Zhou, and S.N. Schiffres, *Addit. Manuf.* 32, 100996 (2020).
14. J. Dawes, R. Bowerman, and R. Trepleton, *Johns Matthey Technol Rev* 59(3), 243 (2015).
15. L.V.M. Antony, and R.G. Reddy, *JOM* 55(3), 14 (2003).
16. M.Z. Gao, B. Ludwig, and T.A. Palmer, *Powder Technol.* 383, 30 (2021).
17. M. Boisvert, D. Christopherson, P. Beaulieu, and G. L'Espérance, *Mater. Des.* 116, 644 (2017).
18. S. Hoeges, A. Zwiren, and C. Schade, *Met. Powder Rep.* 72(2), 111 (2017).
19. E. Olson, *J. GXP Compliance* 3(15), 85 (2011).
20. J.A. Slotwinski, E.J. Garboczi, P.E. Stutzman, C.F. Ferraris, S.S. Watson, and M.A. Peltz, *J. Res. Natl. Inst. Stand. Technol.* 119, 460 (2014).
21. S.J. Blott, and K. Pye, *Sedimentology* 55(1), 31 (2008).
22. A.B. Spierings, M. Voegtlin, T. Bauer, and K. Wegener, *Prog. Addit. Manuf.* 1(1–2), 92016).
23. ASTM Standard B417, *Standard Test Method for Apparent Density of Non-Free-Flowing Metal Powders Using the Carney Funnel* (ASTM International, West Conshohocken, 2018).
24. O. Macho, K. Demková, Ľ Gabrišová, M. Čierny, J. Mužíková, P. Galbavá, Ž Nižnanská, J. Blaško, P. Peciar, R. Fekete, and M. Peciar, *Acta Polytech.* 60(1), 732020).

25. "REVOLUTION Powder Analyzer | Mercury Scientific Inc." [Online]. Available: http://www.mercuryscientific.com/instruments/revolution-powder-analyzer.
26. M. Soltaninejad, M. Soltaninejad, K.F. Saberi, M.K. Moshizi, V. Sadeghi, and P. Jahanbakhsh, *Clean Technol. Environ Policy* 2021(1), 1 (2021).
27. S. Karnati, J. Hoerchler, F. Liou, and J. Newkirk, Available: https://scholarsmine.mst.edu/mec_aereng_facwork/4381 (2017).
28. Horiba Instrument Catalog, *Horiba Instrum. Cat.*, 1, (2014).
29. H. Chen, Q. Wei, Y. Zhang, F. Chen, Y. Shi, and W. Yan, *Acta Mater.* 179, 158 (2019).